



Inter-comparison of two high-accuracy fast-response spectroscopic sensors of carbon dioxide: a case study

B. A. Flowers, H. H. Powers, M. K. Dubey, and N. G. McDowell

Earth and Environmental Science Division, Los Alamos National Laboratory, Los Alamos, NM 87545, USA

Correspondence to: M. K. Dubey (dubey@lanl.gov)

Received: 6 September 2011 – Published in Atmos. Meas. Tech. Discuss.: 15 September 2011

Revised: 29 March 2012 – Accepted: 30 March 2012 – Published: 8 May 2012

Abstract. Tunable diode laser absorption (TDL) and cavity ring-down spectroscopic (CRDS) sensors for atmospheric carbon dioxide were co-deployed during summer and fall of 2010 in field and laboratory conditions at Los Alamos National Laboratory. Both sensors were characterized for accuracy and precision for ambient carbon dioxide measurements at ground level and compared using both laboratory and ambient field data. After post-processing that included water vapor correction and calibration to WMO reference standards, overall mean $[^{12}\text{C}^{16}\text{O}_2] = 392.05 \pm 8.92$ ppm and $[^{12}\text{C}^{16}\text{O}_2] = 392.22 \pm 9.05$ ppm were observed between 29 July and 16 August 2010. The mean difference between the CRDS and TDL data for $^{12}\text{CO}_2$ was 0.04 ± 1.80 ppm ($\pm 1\sigma$ in 60 s) for ambient field data, demonstrating the sensors meet the WMO/IAEA compatibility standard. The observations show over the 19-day period the $[\text{CO}_2]_{\text{CRDS}}/[\text{CO}_2]_{\text{TDL}}$ ratio exhibits a Gaussian distribution centered at $x_0 = 1.003 \pm 3.38 \times 10^{-5}$ ($\pm 1\sigma$), indicating the ratio is dominated by random noise as opposed to a bias in the output of either sensor. The CRDS sensor is capable of measuring $[^{12}\text{C}^{16}\text{O}_2]$ to a precision of 23 ppb in 1 min and decreases to 6.5 ppb in 58 min. At one and 58-min, the TDL exhibits precisions of 29 ppb and 53 ppb. The CRDS is compact, fast, and stable; the TDL is larger and requires frequent calibrations to maintain its precision. The sensors also exhibit consistent hourly averaged diurnal values underscoring the interplay of biological, anthropogenic, and transport processes regulating CO_2 at the site.

1 Introduction

Sensors based on optical spectroscopy are important tools for rapid, accurate in situ measurements of greenhouse gases for biosphere-atmosphere flux estimates and source attribution applications. Sensors using mid-IR and IR laser sources or high finesse optical cavities are the state of the art for continuously sensing greenhouse gases with high precision and temporal resolution (Brown, 2003; Chen et al., 2010; Karlon et al., 2010). Numerous laser-based sensors are undergoing rapid development to study greenhouse gases, thus it is important to conduct instrument inter-comparisons to establish their compatibility under field conditions. The World Meteorological Organization/International Atomic Energy Agency recommends laboratory inter-comparison compatibility of ± 0.1 ppm for total CO_2 and further recommends that CO_2 mixing ratios be reported for dry gases (WMO, 2009).

We inter-compare a commercially available cavity ring-down absorption analyzer (CRDS) with a commercially available tunable diode laser absorption (TDL) system for monitoring carbon dioxide $[^{12}\text{C}^{16}\text{O}_2]$. Both the CRDS and TDL sensors are used throughout the climate and ecosystem research and environmental sensing communities and it is important to directly compare the results of laser-based optical absorption sensors operating via related principles but different techniques to ensure data sets from either sensor are in agreement with reference standards and each other.

The purpose of this paper is to compare $[^{12}\text{C}^{16}\text{O}_2]$ obtained operating the CRDS and TDL sensors under their optimal operational protocols. We conducted the study in both the laboratory and field settings to establish accuracy and precision for the two sensors. In the laboratory, the CRDS and TDL were tested against the same standard gas mixtures

(CO₂ in air, dried to -45°C dew point). In the field, we compared the ambient carbon dioxide data sets obtained from the sensors obtained during a nineteen-day period in late summer 2010. For ambient measurements, the CRDS analyzer and TDL sensors were set up at the same field site and run on a common inlet and controlled by their respective sampling protocols.

2 Methods

The carbon dioxide sensors used in this study are a cavity ring-down analyzer (Picarro 1301-m, Picarro, Inc. CA, USA) (Crosson, 2008) and a TDL absorption sensor (TGA100, Campbell Scientific, Logan, UT). The CRDS sensor measures $^{12}\text{C}^{16}\text{O}_2$, $^{12}\text{C}^{1}\text{H}_4$, and $^1\text{H}_2^{16}\text{O}$ while the TDL sensor measures isotopologues of CO₂: $^{12}\text{C}^{16}\text{O}_2$, $^{13}\text{C}^{16}\text{O}_2$, $^{18}\text{O}^{12}\text{C}^{16}\text{O}$ by direct absorption near 2309 cm^{-1} (Bowling et al., 2003). For direct comparison, only the $^{12}\text{C}^{16}\text{O}_2$ signals from either instrument are used in this work and are referred to as CO₂ hereafter. Both the CRDS and TDL instruments have been described previously (e.g., Crosson, 2008; Bowling, et al., 2003) and the TDL sensor used in this study has been described in (Powers et al., 2010). The CRDS sensor uses a near-IR diode laser (scanned between 1603 and 1641 nm to cover CO₂ and CH₄ bands) that does not require liquid nitrogen cooling. Nominal conditions are controlled inside the CRDS optical cavity; measured over the 19 day study to be ($P = 139.899 \pm 0.068$ Torr, $T = 45.000 \pm 0.002^{\circ}\text{C}$), leading to stable spectroscopic features largely devoid of pressure broadening effects. Similarly, the CRDS sensor does not require frequent in situ absorption response calibrations, which are essential for the TDL sensor. The CRDS sensor is designed to operate without in situ calibration on ambient air, particulate matter is filtered from the sampled gas stream but no drying is performed. Water vapor can interfere with the accuracy of CO₂ and CH₄ measured with the CRDS due to its operation in the near-IR. Additionally, the WMO recommends GHG gas measurements be reported for dry mixing ratios. Therefore the effects of water vapor on the CRDS performance are of special concern. The response of the CRDS sensor to water vapor has been documented (Rella, 2010; Chen et al., 2010) and the procedures recommended by the manufacturer in their 2010 white paper (Rella, 2010) have been used here to produce dry mixing ratios of carbon dioxide used for the inter-comparison. Water vapor affects the accuracy of the water, methane, and carbon dioxide concentrations reported by CRDS sensor and the post-processing corrections for water vapor interference in all three channels are given below.

$$\text{H}_2\text{O}_{\text{actual}} = 0.772 \times (\text{H}_2\text{O}_{\text{CRDS}} + 0.02525 \times \text{H}_2\text{O}_{\text{CRDS}}^2) \quad (1)$$

$$\text{CO}_{2,\text{dry}} = \frac{\text{CO}_{2,\text{CRDS}}}{1 + (-0.012 \times \text{H}_2\text{O}_{\text{CRDS}}) + (-2.67 \times 10^{-4} \times \text{H}_2\text{O}_{\text{CRDS}}^2)} \quad (2)$$

$$\text{CH}_{4,\text{dry}} = \frac{\text{CH}_{4,\text{CRDS}}}{1 + (-0.00982 \times \text{H}_2\text{O}_{\text{CRDS}}) + (-2.393 \times 10^{-4} \times \text{H}_2\text{O}_{\text{CRDS}}^2)} \quad (3)$$

The suitability of the above equations for water vapor corrections to the H₂O, CH₄, and CO₂ data produced by the CRDS sensor are vetted by both (Chen et al., 2010; Rella, 2010).

The TDL sensor uses a liquid nitrogen cooled tunable lead-salt diode laser that measures $^{12}\text{CO}_2$ absorption near 2308.225 cm^{-1} . Pressure and temperature in the TDL optical cavity were maintained at 15.0 Torr and 30°C respectively. The TDL sensor is calibrated frequently, the operational cycle is ambient air is sampled for 60 s, then a high concentration reference gas for 30 s, then a low concentration reference gas for 30 s. The first 15 s of each measurement in the cycle are not used in the data analysis to account for flushing of the TDL optical cell. The high and low reference gases were tertiary calibration standards cross referenced with WMO-traceable standards from NOAA-ESRL using the TDL. The TDL routinely operates using these tertiary standards to conserve the WMO standards over time. The WMO reference gases were sourced from and calibrated by the NOAA Greenhouse Gases Group at the Global Monitoring Division. The uncertainties in the WMO reference concentrations are the standard deviations reported by the above laboratory. The TDL was calibrated using a linear regression between the reference gases bracketing the CO₂ concentration of any samples run. The TDL responses to the high and low reference gases are held constant in the linear regression to determine sampled [CO₂]. Particulate matter is filtered from the TDL sample stream and is dried with a Nafion drying system so that the humidity of the sampled gas stream is approximately the same humidity as the reference gases. The TDL sensor operates in the mid-IR and the fundamental CO₂ vibrational features used for detection are well separated from those of water.

Both sensors were housed at a semi-arid pinon-juniper (*juniperus monosperma*) woodland site with low vegetation density at the Los Alamos National Laboratories' Environmental Research Park (Shim et al., 2011). The laboratory that housed the sensors was temperature controlled at 70 F during both ambient and laboratory measurement. The average canopy height is 3.5 m. For ambient monitoring, air was sampled approximately 5 meters above ground outside a laboratory that is surrounded by the woodland for $\sim 74\text{ km}^2$. Both the CRDS and TDL sensors sampled ambient air from a single tube that was run out of the building to a small tower. The tube was connected to a manifold and the CRDS and TDL sensors sampled from the manifold continuously at 500 ml min^{-1} and 200 ml min^{-1} respectively. The sensors were run independently of each other, using their own operational sampling protocols. The CRDS sensor was operated without in situ calibration for the 19-day study. In the TDL

protocol, the sample stream was switched to both a high or low reference calibration gas for 30 s, then measured ambient $[\text{CO}_2]$ for 1 min. The first 15 s of data at each stage of this cycle is ignored to account for flushing and sample equilibration in the TDL optical cavity (Powers et al., 2010), minimizing the difference of cavity volumes and sampling rates on the inter-comparison statistics.

3 Results and discussion

3.1 Laboratory inter-comparison and instrumental precision

For the laboratory inter-comparison, the CRDS sensor was plumbed into the manifold that controls the previously described automated sampling and calibration protocol for the TDL sensor. Automated cycling between high, low, and unknown gases was performed for 16 h and output for the CRDS and TDL sensors were averaged to 1 min time constants. For the TDL, the enforced high and low reference concentrations were 557.6 ± 0.1 ppm for $[\text{CO}_2]_{\text{high}}$ and 354.6 ± 0.1 ppm for $[\text{CO}_2]_{\text{low}}$ were used and the measured response to the unknown sample was measured $[\text{CO}_2]_{\text{unknown}} = 407.835 \pm 0.091$ ppm, a percent relative standard deviation (% RSD) = 0.02 % for $[\text{CO}_2]_{\text{unknown}}$. The response for the CRDS sensor was $[\text{CO}_2]_{\text{high}} = 547.707 \pm 0.743$ ppm, $[\text{CO}_2]_{\text{low}} = 352.829 \pm 0.076$ ppm, and $[\text{CO}_2]_{\text{unknown}} = 405.923 \pm 0.121$ ppm, respectively (CRDS % RSD = 0.1 %, 0.02 %, and 0.03 % respectively for the high, low, and unknown samples). The CRDS sensor responded to “zero-air” (ambient air passed through a soda-lime CO_2 scrubber) $[\text{CO}_2]_0 = -0.02 \pm 0.03$ ppm over several hours of operation prior to beginning the inter-comparison experiments. The TDL sensor is not recommended to be operated in absence of CO_2 . The high and low TDL responses are programmed to the values of the CO_2 tanks prescribed by the NOAA laboratory, so we enforced a (0,0) point in the calibration plot and enforced the fit through the origin of the calibration plot. Prior to this, the linear regression exhibited a slope of 0.985 and an offset of 1.43. This offset is not statistically different from zero. The $[\text{CO}_2]$ values for the laboratory calibration are plotted in Fig. 1 and the slope of the linear regression between the CRDS and TDL response to the reference and unknown tanks is the CRDS calibration factor, $f_{\text{CRDS}} = 0.989 \pm 0.004$ ($r^2 = 0.999$ for the regression analysis). This inter-comparison calibrates the CRDS response to the WMO reference standards. The ($\pm 1\sigma$) standard deviations for each concentration are used as error bars, but are too small to see in the plot. The calibration factor is based on reference standards known to a higher precision (sub ppm compared with a few ppm) and wider concentration range than previously used by our group for the CRDS sensor. We use the f_{CRDS} calibration factor determined from

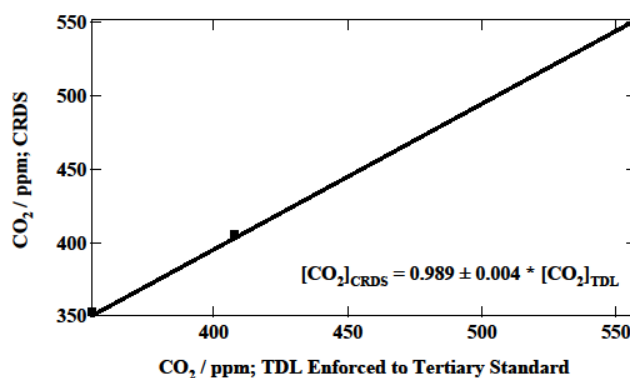


Fig. 1. Laboratory calibration plot of CRDS sensor with TDL tertiary standards showing linear response of the CRDS to reference gases between 375 and 560 ppm CO_2 .

high precision tertiary standards to correct ambient concentrations: $\times [\text{CO}_2]_{\text{CRDS}} = [\text{CO}_2]_{\text{CRDS}}$. Post-calibrated CRDS data is used for inter-comparison with the TDL for both the laboratory and ambient data sets. The WMO/IAEA metric for compatibility between two instruments is that they agree to ± 0.1 ppm for total CO_2 .

We use the laboratory inter-comparison study to establish the precision and stability as a function of signal integration time for the CRDS and TDL measurement methods using the Allan variance technique (Werle et al., 1993). When the overall noise is dominated by random noise, increasing signal integration time decreases the variance (σ^2) until a time at which instrumental noise begins to dominate and the variance begins to increase. The maximum precision of each sensor is defined at the integration time where the signal variance is minimized. The transition between random and instrumental noise can be sharp (quick) or shallow (long), demonstrated in Bowling et al. (2003) and Tuzson et al. (2010). We perform this analysis to compare the performance of the CRDS and TDL measuring a reference gas. We note the TDL is calibrated for 30 s each at high and low standards and measures the sample gas for 60 s. In contrast, the CRDS is not constantly re-calibrated and data is reported every ~ 0.75 s. This is apparent in the time scales of the Allan variance plot, where the CRDS data begins at 1 s (black trace) and at 15 s for the TDL (red trace). Using 16 h of data at $[\text{CO}_2] = 405.923 \pm 0.121$ ppm (from the unknown sample tank in the previous section), we estimate the precision of the CRDS sensor to be 29 ppb at 30-s integration and 23 ppb at 60-s integration time. The same statistics for the TDL at 30 and 60 s integration time are 34 ppb and 29 ppb. At 58 min (3500 s integration time), the precision of the CRDS sensor is 6.5 ppb and the same statistic for the TDL is 53 ppb. Figure 2 shows the Allan variance plot for the CRDS (black trace) and TDL (red trace) sensors taken from the laboratory data set. We clearly see the stability of the CRDS sensor does not show a sharp “V” shape as exhibited in Allan variance

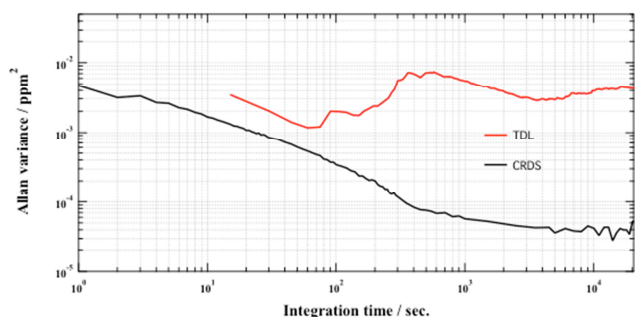


Fig. 2. Allan variance plot for CRDS sensor (black trace) and TDL (red trace) for 16 h of data shown as a log-log plot of signal variance vs. signal integration time. The minimum variance is observed at 58-min signal integration time for the CRDS sensor and at 60 s for the TDL sensor.

plots for the TDL but a slower transition from the so-called white noise to drift noise regions of the Allan variance plot (Werle et al., 1993). The local variance minimum at 2 s in the CRDS trace is repeatable noise in the variance data, and we do not interpret this as a variance minimum at which instrumental precision should be prescribed (Werle, 2010). This behavior is similarly exhibited by the quantum cascade laser absorption spectrometer (QCLAS) methane sensors described by (Tuzson et al., 2010). The CRDS sensor exhibits stability at considerably longer integration times than does the TDL sensor, the minimum detection limit (6.5 ppb) is observed at 3500 s (58 min) signal integration time, opposed to 30 s (23 ppb) for the TDL, which corresponds to two calibration cycles in its measurement protocol. The CRDS detection limit at 58 min is in close agreement with the prototype CRDS sensor from the manufacturer (A. D. Van Pelt, personal communication, 2011), and is here independently verified.

3.2 Continuous ambient carbon dioxide monitoring

We characterize the agreement between the two sensors for quantitative CO₂ measurement for ambient field air by comparing their temporal relationships; the linear regression between their temporal signals, and the calculated ratio and difference for their response to ambient CO₂ for the 19 day observation period. The 1-min temporal response of both sensors to ambient CO₂ near Los Alamos, NM is shown in Fig. 3. The [CO₂]_{CRDS} mixing ratio is shown on top, [CO₂]_{TDL} is shown on the bottom of the plot. The ambient [CO₂] signal varies between 378 and 440 ppm. The diurnal variation is ~60 ppm day⁻¹ at ground level. Linear regression analysis between [CO₂]_{CRDS} and [CO₂]_{TDL} is shown in Fig. 4. The linear regression analysis of the 1-min averaged signal between the sensors yields [CO₂]_{CRDS} = 1.00 ± 1.7 × 10⁻³ [CO₂]_{TDL} + (2.41 ± 0.66) with R² = 0.96 for the ambient data. Assuming a zero offset (i.e., perfect agreement)

between the CRDS and TDL sensors, the linear regression between the CRDS and TDL ambient data sets results in [CO₂]_{CRDS} = 1.00 ± 3.8 × 10⁻⁵ [CO₂]_{TDL}. The mean ratio calculated [CO₂]_{CRDS}/[CO₂]_{TDL} for the sampling period is 1.000 ± 0.005. Also shown in Fig. 4 is a histogram of the ratio [CO₂]_{CRDS}/[CO₂]_{TDL} for the 1-min data. The peak of the gaussian fit to the histogram data is centered at x₀ = 1.003 ± 3.28 × 10⁻⁵. We note the importance of synchronizing the time axis for proper inter-comparison between the two sensors. For example, on 16 August 2010 there was some drifting (both forward and backward) between the clocks on CRDS and TDL analyzers. The data had to be separated into periods that exhibited linear time relationships between the time stamps of either sensor, analyzed for correlation separately by matching peak features in the subset time series, and subsequently concatenated together. Originally the correlation analysis for 16 August showed [CO₂]_{CRDS} = 0.979 ± 0.008 [CO₂]_{TDL} + (13.10 ± 2.95), a y-intercept that is statistically different from zero (and indeed may be interpreted as a 13 ppm offset in [CO₂]_{CRDS}). The data on 16 August was separated into AM and PM periods and time synchronized separately. This data was merged and re-analyzed to [CO₂]_{CRDS} = 1.003 ± 0.007 [CO₂]_{TDL} + (3.67 ± 2.6), which we interpret as a zero-intercept with respect to a quantitative [CO₂] offset between the two sensors.

The final trace in Fig. 3 is the self-corrected ambient water ([H₂O]_{dry}) measured during the ambient observations. The maximum volume percent observed throughout the measurement period was 2.7 % and the minimum was 0.66 %. The mean self-corrected ([H₂O]_{dry}) observed was 1.58 ± 0.34 % by volume. We observed no correlation between the 1-min difference between the CRDS-TDL sensors (ΔCO₂) vs. ([H₂O]_{dry}). The water vapor correction reported by Rella (2010) is observed robust in this case study. The difference between the post-calibrated CRDS and TDL signals is the key statistic for the inter-comparison analysis described here. The mean difference between [CO₂]_{CRDS} and [CO₂]_{TDL} is 0.04 ppm ± 1.80 ppm (±1σ) for the 1-min time averaged data (plotted as the third trace in Fig. 3). The mean difference is less than the ±0.100 ppm metric set forth by the WMO/IAEA, hence we have demonstrated that on average the ambient air CO₂ results from the CRDS and TDL sensors are compatible when the sensors are calibrated to high precision standards and the CRDS signal is corrected for water vapor interference.

3.3 Diurnal cycle of carbon dioxide

The laboratory calibration and 1-min time resolution agreement between the data sets are robust factors underlying longer time averaged data to describe the diurnal pattern of the [CO₂] atmospheric background signal. The hourly averaged diurnal pattern of CO₂ is an important statistic to understand local biogenic respiration/photosynthesis processes

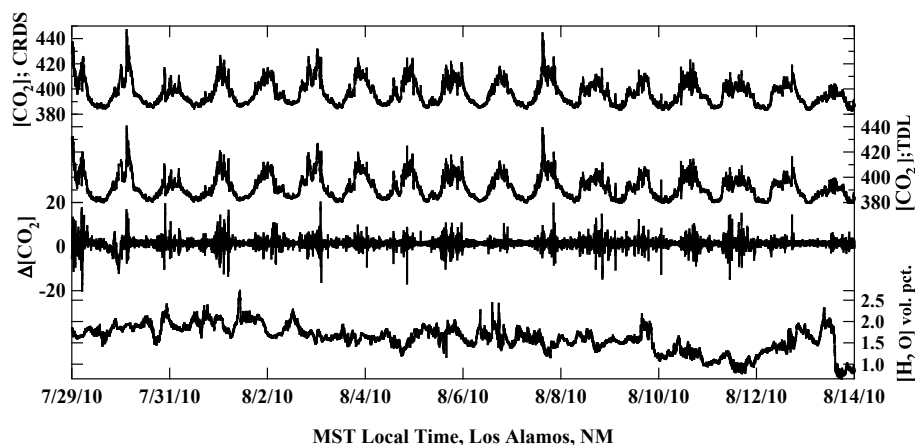


Fig. 3. Temporal profile of $^{12}\text{C}^{16}\text{O}_2$ mixing ratio measured near Los Alamos, NM with CRDS and TDL sensors. The CRDS signal has been cross-calibrated, as described in the text. The $\Delta[\text{CO}_2]$ trace shows the temporal profile of the $[\text{CO}_2]_{\text{CRDS}} - [\text{CO}_2]_{\text{TDL}}$ difference.

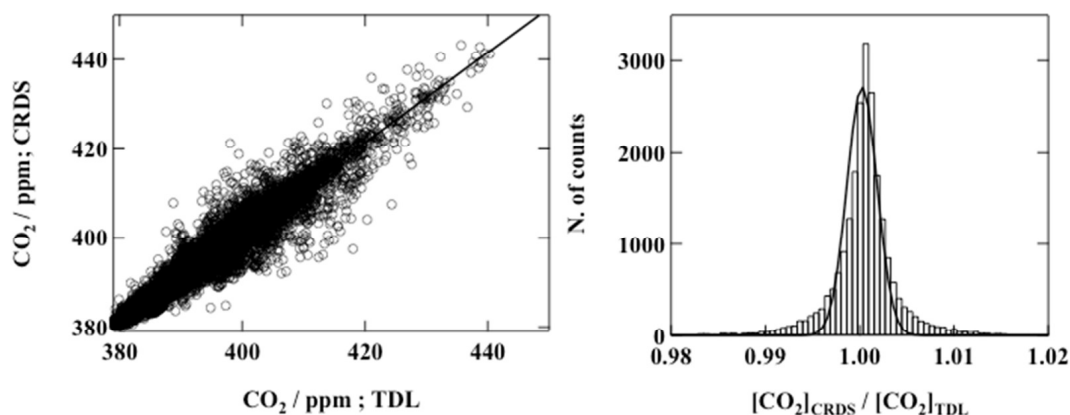


Fig. 4. Linear regression analysis of $^{12}\text{C}^{16}\text{O}_2$ measured with commercial CRDS and TDL analyzers after cross calibration using 1-min time resolution. The linear regression analysis between the CRDS and TDL response is $[\text{CO}_2]_{\text{CRDS}} = 1.000 \pm 3.30 \times 10^{-5} [\text{CO}_2]_{\text{TDL}}$; $r^2 = 0.96$. The histogram plot of the ratio between the CRDS and TDL measurements and the gaussian fit of the $[\text{CO}_2]_{\text{CRDS}}/[\text{CO}_2]_{\text{TDL}}$ ratio is centered on an x_0 value of 1.003.

and effects transport (including anthropogenic CO_2) in the regional CO_2 background. Raw data was averaged to 1-h time constants for each hour of the day (0–23 h) for the 19-day ambient observation study to create hourly averaged diurnal CO_2 profiles. Table 1 shows the median diurnal $[\text{CO}_2]$ for each hour (60 min averaged) of the day between 29 July and 16 August 2010 from the CRDS (top trace) and TDL (bottom trace) sensor. Nightly increases (00:00–06:00 and 20:00–23:00 LT – local time) in $[\text{CO}_2]$ (both in magnitude and variability) are due to respiration and daily (07:00–19:00 LT) uptake of $[\text{CO}_2]$ by photosynthesis is evident in data sets from both sensors. Ambient temperature is included in the third column. The fourth column in Table 1 shows the difference between the diurnal median $[\text{CO}_2]$ for each hour. The mean difference between the CRDS and TDL diurnal median 1-h values is much smaller (1.80 ± 1.50) ppm than either of their variabilities (difference between 75th and

25th percentiles), 4.85 ± 2.40 ppm and 5.17 ± 2.56 ppm for CRDS and TDL respectively. The correlation factor (r^2) between the $[\text{CO}_2]$ data sets is 0.91, a correlation factor of 1.0 represents a perfectly correlated relationship. Anti-correlation between median diurnal ambient temperature and median diurnal $[\text{CO}_2]$ for both sensors is shown in Fig. 5. While the mechanisms controlling this interplay of respiration, photosynthesis, and dynamics are not the subject of our paper, it is clear that both sensors provide very consistent information.

The CRDS system in this study provides robust performance for $^{12}\text{C}^{16}\text{O}_2$, $^{12}\text{C}^{1}\text{H}_4$, and $^1\text{H}_2^{16}\text{O}$ monitoring and is readily deployable to field sites and mobile platforms including aircraft. There is no isotopic speciation data available from this particular CRDS sensor, however it does measure CH_4 and a new version of the sensor includes CO measurement. The TDL system used here is designed to determine

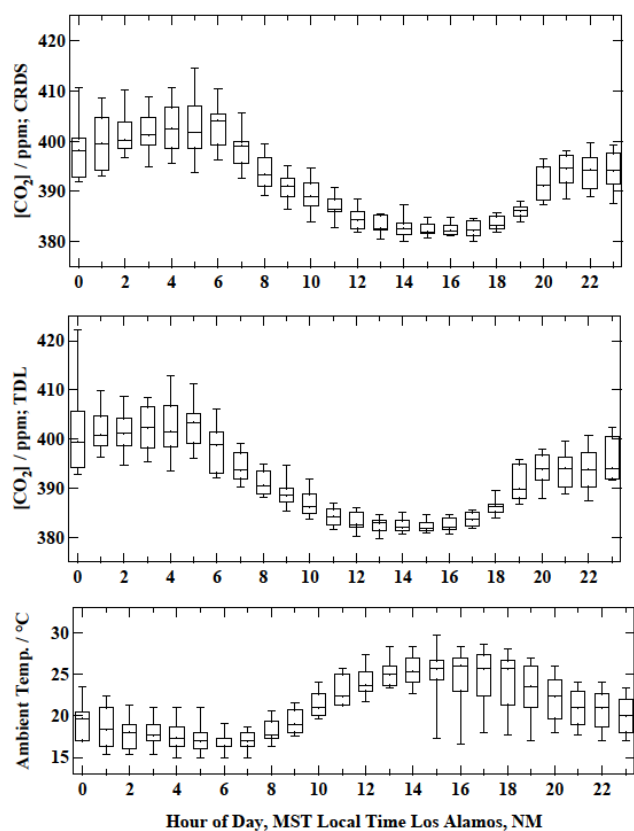


Fig. 5. Hourly diurnal median $[\text{CO}_2]$ between 29 July and 16 August 2010 near Los Alamos NM. The scaled CRDS $[\text{CO}_2]_{\text{CRDS}}$ trace is plotted on top, the $[\text{CO}_2]_{\text{TDL}}$ trace is plotted in the middle and hourly diurnal median ambient air temperature is plotted on the bottom trace.

$\delta^{13}\text{C}$ and $\delta^{18}\text{O}$ ratios in CO_2 at stationary sites. The TDL is capable of measuring 99.91 % of the naturally occurring gaseous CO_2 isotopes and monitoring the $\delta^{13}\text{C}$ and $\delta^{18}\text{O}$ ratios in CO_2 as tracers of air mass history and soil-atmosphere exchange (Pataki et al., 2006; Shim et al., 2011; Powers et al., 2010). However, it is large and requires liquid N_2 cooling and regular calibration making it less ideal for mobile applications.

4 Conclusions

We report the results of a field and laboratory inter-comparison experiment between two commercially available spectroscopic carbon dioxide ($^{12}\text{C}^{16}\text{O}_2$) sensors. Prior to the field inter-comparison, the CRDS sensor was calibrated to two WMO reference standards for CO_2 in a 3-point calibration curve ($m=0.989$, $r^2=0.999$). Over a nineteen-day period, after post calibration, the agreement between the two sensors was quite good (slope=1.000, zero intercept enforced or $[\text{CO}_2]_{\text{CRDS}} = 1.00 \pm 1.7 \times 10^{-3} [\text{CO}_2]_{\text{TDL}} + (2.41 \pm 0.66)$) for 1 min measurements of

Table 1. Hourly diurnal median $[\text{CO}_2]_{\text{CRDS}}$, $[\text{CO}_2]_{\text{TDL}}$, ambient temperature ($^{\circ}\text{C}$), and the absolute value of $\Delta[\text{CO}_2]$ (CRDS–TDL) measured between 29 July and 16 August 2010 near Los Alamos, NM.

Hour	$[\text{CO}_2]_{\text{CRDS}}$	$[\text{CO}_2]_{\text{TDL}}$	Temp. ($^{\circ}\text{C}$)	$\Delta[\text{CO}_2]$
0	398.20	399.41	19.6	1.21
1	399.50	400.98	18.3	1.30
2	400.15	401.18	18.0	1.02
3	401.28	402.30	17.7	1.02
4	402.54	401.53	17.3	1.01
5	401.77	403.41	17.0	1.64
6	404.10	398.86	16.3	5.23
7	399.10	393.67	17.0	5.41
8	393.37	390.47	17.7	2.90
9	391.07	388.55	19.0	2.52
10	388.97	386.19	21.0	2.78
11	386.35	384.21	22.3	2.14
12	384.35	382.59	23.7	1.75
13	382.67	382.89	25.0	0.22
14	382.66	381.94	25.3	0.72
15	381.97	381.75	25.7	0.22
16	382.13	381.96	26.0	0.17
17	382.28	383.62	25.7	1.34
18	383.23	386.25	25.7	3.02
19	391.12	389.83	23.5	3.71
20	391.23	393.85	22.3	2.62
21	394.66	394.06	21.0	0.60
22	394.34	393.83	21.0	0.51
23	394.13	394.04	20.0	0.09
mean	391.55 ± 7.52	391.92 ± 7.66		1.80 ± 1.50

ambient carbon dioxide. Both sensors were observed to behave linearly over a range of ambient $[\text{CO}_2]$ (380–450 ppm) and in laboratory (354–557 ppm). The robust agreement between these sensors underscores their fast, quantitative $[\text{CO}_2]$ capability for atmosphere-biosphere exchange and ambient carbon dioxide (ground, mobile, and flight) measurements. The compatibility of the two data sets was judged as the the mean difference between $[\text{CO}_2]_{\text{CRDS}}$ and $[\text{CO}_2]_{\text{TDL}}$ and was 0.04 ± 1.8 ppm ($\pm 1\sigma$) for dry gas $[\text{CO}_2]$ ambient measurement, hence we demonstrate that the CRDS and TDL instruments are in agreement with the WMO/IAEA compatibility recommendation of ± 0.100 ppm for dry $[\text{CO}_2]$. A gaussian fit to the histogram of the $[\text{CO}_2]_{\text{CRDS}}/[\text{CO}_2]_{\text{TDL}}$ ratio over the 19 day observation was centered at $1.003 \pm 3.38 \times 10^{-5}$ ($\pm 1\sigma$). The precisions for the sensors were determined from statistical analysis from 16 h of data taken from a single CO_2 source. The agreement between the water vapor corrected CRDS and the TDL (which is unaffected by water vapor interference) is an independent verification of the validity of the water vapor correction applied to the CRDS data. At 1 min, the TDL exhibited its maximum precision (minimum variance)

of 29 ppb and the CRDS shows a comparable precision of 23 ppb. We observed the minimum variance of the CRDS CO₂ response after 58 min of signal integration. At 58 min time constants, we observed TDL precision of 53 ppb and 6.5 ppb for the CRDS sensor.

Operational in situ calibration of the CRDS system is needed infrequently (especially for ground based sensing), but periodic calibration with high precision standards should be performed to ensure linearity of its response under ambient [CO₂] conditions. Both sensors provide valuable data for carbon dioxide monitoring and their additional data streams put the CO₂ data stream in different contexts, i.e., H₂O, CO₂, and CH₄ from the CRDS and ¹²C¹⁶O₂, ¹³C¹⁶O₂ and ¹⁸O¹²C¹⁶O from the TDL. Inter-comparison for isotopic speciation sensors (e.g., ¹³C¹⁶O₂ and ¹⁸O¹²C¹⁶O) should be investigated for appropriate sensors to judge their compatibility according to WMO/IAEA standards. Our study will be especially valuable for analysis of experiments where multiple high precision fast response instruments are measuring greenhouse gases and differences may need to be interpreted and diagnosed (Wofsy, 2011).

Acknowledgements. B. A. F. and M. K. D. acknowledge the US Department of Energy ASR program and LANL's Laboratory Directed Research and Development program (LDRD). H. P. and N. M. acknowledge Cliff Meyer, LANL's LDRD program and the Institute for Geophysical and Planetary Physics (IGPP) Programs.

Edited by: M. von Hobe

References

- Bowling, K., Sargent, S. D., Tanner, B. D., and Ehleringer, J. R.: Tunable diode laser absorption spectroscopy for stable isotope studies of ecosystem-atmosphere CO₂ exchange, *Agr. Forest Meteorol.*, 118, 1–19, 2003.
- Brown, S. S.: Absorption Spectroscopy in High-Finesse Cavities for Atmospheric Studies, *Chem. Rev.*, 103, 5219–5238, doi:10.1021/cr020645c, 2003.
- Chen, H., Winderlich, J., Gerbig, C., Hofer, A., Rella, C. W., Crosson, E. R., Van Pelt, A. D., Steinbach, J., Kolle, O., Beck, V., Daube, B. C., Gottlieb, E. W., Chow, V. Y., Santoni, G. W., and Wofsy, S. C.: High-accuracy continuous airborne measurements of greenhouse gases (CO₂ and CH₄) using the cavity ring-down spectroscopy (CRDS) technique, *Atmos. Meas. Tech.*, 3, 375–386, doi:10.5194/amt-3-375-2010, 2010.
- Crosson, E. R.: A cavity ring-down analyzer for measuring atmospheric levels of methane, carbon dioxide, and water vapor, *Appl. Phys. B*, 92, 403–408, 2008.
- Karlon, A., Sweeney, C., Tans, P., and Newberger, T.: AirCore: An Innovative Atmospheric Sampling System, *J. Atmos. Ocean. Tech.*, 27, 1839–1852, 2010.
- Pataki, D. E., Bowling, D. R., Ehleringer, J. R., and Zobitz, J. M.: High resolution atmospheric monitoring of urban carbon dioxide sources, *Geophys. Res. Lett.*, 33, L03813, doi:10.1029/2005GL024822, 2006.
- Powers, H. H., Hunt, J. E., Hanson, D. T., and McDowell, N. G.: A dynamic soil chamber system coupled with a tunable diode laser for online measurements of δ¹³C, δ¹⁸O, and efflux rate of soil-respired CO₂, *Rapid Commun. Mass Spectrom.*, 24, 243–253, 2010.
- Rella, C.: Accurate Greenhouse Gas Measurements in Humid Gas Streams Using the Picarro G1301 Carbon Dioxide/Methane/Water Vapor Gas Analyzer, Sunnyvale, CA, 2010.
- Shim, J., Powers, H. H., Meyer, C., Pockman, W., and McDowell, N.: The role of inter-annual, seasonal, and synoptic climate on the carbon isotope ratio of ecosystem respiration at a semi-arid woodland, *Global Change Biol.*, 17, 2584–2600, doi:10.1111/j.1365-2486.2011.02454.x, 2011.
- Tuzson, B., Hiller, R. V., Zeyer, K., Eugster, W., Neftel, A., Ammann, C., and Emmenegger, L.: Field intercomparison of two optical analyzers for CH₄ eddy covariance flux measurements, *Atmos. Meas. Tech.*, 3, 1519–1531, doi:10.5194/amt-3-1519-2010, 2010.
- Werle, P.: Time domain characterization of micrometeorological data based on a two sample variance, *Agr. Forest Meteorol.*, 150, 832–840, 2010.
- Werle, P., Mücke, R., and Slemr, F.: The Limits of Signal Averaging in Atmospheric Trace-Gas Monitoring by Tunable Diode-Laser Absorption Spectroscopy (TDLAS), *Appl. Phys. B*, 57, 131–139, 1993.
- WMO: 15th WMO/IAEA Meeting of Experts on Carbon Dioxide, Other Greenhouse Gases and Related Tracers Measurements Techniques, Jena, Germany, 2009.
- Wofsy, S. C.: HIAPER Pole-to-Pole Observations (HIPPO): fine-grained, global-scale measurements of climatically important atmospheric gases and aerosols, *Philos. T. Roy. Soc. A*, 369, 2073–2086, 2011.